
Article:
Sediq, K.N., Coles, D., Fry, P.W. et al. (1 more author) (2016) Plasmonic gold nanodiscs fabricated into a photonic-crystal nanocavity. Nanotechnology, 27 (22). p. 225203. ISSN 0957-4484

https://doi.org/10.1088/0957-4484/27/22/225203

Plasmonic gold nanodiscs fabricated into a photonic-crystal nanocavity

Khalid N. Sediq[a], David Coles[b], Paul W. Fry[c] and David G. Lidzey*[a]

[a] Department of Physics and Astronomy, University of Sheffield, Sheffield, S3 7RH, United Kingdom

[b] Department of Materials, Hume-Rothery Building, University of Oxford, Parks Road, Oxford, OX1 3PH, United Kingdom

[c] Centre for Nanoscience and Technology, North Campus, Broad Lane, Sheffield, S3 7HQ, United Kingdom

* Corresponding author: d.g.lidzey@sheffield.ac.uk

Abstract

We fabricate and characterise an optical structure consisting of a photonic crystal L3 nanocavity containing two gold nanodisks placed close to a field antinode. We use finite difference time domain (FDTD) modelling to show that the optical properties of the nanocavity are sensitive to the physical separation between the gold nanodisks, and that at reduced separation, the q-factor of a cavity mode polarised parallel to the dimer long-axis is reduced, indicating coupling between the cavity mode and a localised plasmon. Preliminary experimental measurements indeed indicate a damping of the cavity mode in the presence of the dimer; a result consistent with the FDTD modelling. Such a scheme may be used to integrate plasmonic systems into all-optical photonic circuits.

Introduction

When noble metals are structured at the nanoscale, it is possible to engineer structures to support localized surface plasmon resonances (LSPRs). Such LSPRs are associated with the oscillations of collective electrons in the metal conduction band under the influence of an external electromagnetic field [1], and by placing metallic nanoparticles (MNPs) in close proximity, it is possible to significantly enhance electromagnetic fields creating 'hot-spots' Such enhanced fields are of significant interest for their ability to interact with molecular materials, resulting in enhancement in Raman scattering cross-sections [2], leading to a range of applications in bio-sensing [3]. Previous work has shown that the radiation emitted from LSPRs are dependent on their geometry and their orientation with respect to the excitation field [4-6].

There is growing interest in the incorporation of such plasmonic structures into optical cavities that are able to confine light with high efficiency (as measured by the cavity Q-factor). Here, the combination of ultra-small EM-field localisation created by the plasmonic cavity with the ability of an optical cavity to harvest and store light effectively is of interest both for the study of fundamental light-matter coupling effects and for the creation of new types of optoelectronic device. A number of authors have now explored the combination of plasmonic elements with photonic crystal nanocavities [7,8, 11-13]. Here, such structures are based on a membrane in which there is periodic manipulation of local refractive index (forming a photonic crystal), containing a deliberately defined physical defect. Such defects (e.g. missing 'holes' in the photonic crystal) are able to strongly localise light, creating optical resonators having significantly reduced optical loss and thus a very high Q-factor [14-17]. Photonic-crystal optical nanocavities have been widely explored for a number of applications ranging from nano-scale lasers [18] and single-photon light-sources [19] to chemical sensors [20].

Hybrid plasmonic-photonic systems have been demonstrated in various types of structures that have been fabricated using different techniques. For example, colloidal gold nanosphere dimers have been placed into a silicon nitride waveguide using a dip-pen lithography technique [7, 21 22]. Other work has explored the properties of metallic split-ring resonators defined into a Si/SiO_2 based nanocavity structure, with the entire structure fabricated using electron-beam lithography (EBL) [13]. We have previously used a laser printing technique to place a single gold nanoparticle into a SiN based nanocavity [23], however the registration

accuracy of this technique was relatively limited. Recent work has explored the incorporation of 'bow-tie' plasmonic elements into an L7 InP based structure operating at 1.5 μm, with the entire structure fabricated by EBL. Here, the bow-tie element was placed at various places in the cavity to explore coupling between the plasmonic and the optical resonance, and it was shown that the structure was able to undergo optically-pumped lasing [8].

In this paper we report a hybrid plasmonic/photonic crystal system, in which we fabricate a SiN based L3 nanocavity that contains a gold nanodisk dimer, with the entire structure defined using EBL followed by a sequence of etching and subsequent deposition steps. Our cavities operate at optical wavelengths (around 650 nm) and therefore may be able to couple to red / NIR plasmon supported by the nanodisk dimer. We use our approach to explore the effect of the nanoparticle (NP) separation on the wavelength and intensity of cavity mode. Our preliminary measurements are compared with an FDTD model that indicates that a confined cavity mode is able to directly excite the dimer plasmon. We discuss the opportunities for the use of our structures in advanced photonic devices.

Methods

The structures that we have explored are shown schematically in Figure 1(a), with an SEM image of the final structure shown in Figure 1(b). Here, it can be seen that a pair of gold nanodisks having a long-axis of 160 nm, an aspect ratio of 1.53 separated by 40 nm are placed in the centre of an L3 nanocavity (defined into SiN). To create this structure, we coated a 180 nm thick layer of electron-sensitive PMMA resist onto a 200 nm thickness freestanding silicon nitride membrane slab that was then baked at 180°C for 10 minutes to remove solvent and facilitate cross-linking. This PMMA layer was then patterned using EBL to define the eventual location of the metallic dimers. The exposed resist was the developed and removed selectively using a MIBK: IPA developer. The structure was the exposed to an inductively-coupled plasma etch to remove ~ 10 nm of silicon nitride. A thin (< 5 nm) titanium adhesion layer [24], followed by a 100 nm thick layer of gold was then deposited onto the entire structure using thermal evaporation. Finally, a piranha-acid (nitric and hydrochloric acid mixture) solution was used to lift-off the remaining resist, leaving two holes filled with gold. Here, the initial creation of the small holes on the SiN surface was found to be important in securing the gold NPs to the surface, and helped prevent their inadvertent removal during subsequent processing steps.

A two dimensional photonic crystal L3 nanocavity was then fabricated around the gold NPs, again using EBL. Here, the photonic crystal was fabricated into the form of a hexagonal lattice having a lattice constant of 260 nm with a hole size of 142 nm using previously described techniques [17, 20, 23]. The photonic nanocavity consisted of three missing holes in the photonic crystal, defined at the location of the gold NPs, such that the central missing hole coincided with mid-point between the NPs. A series of structures were explored, in which the distance between the dimers was varied from 40, 60, 80 to 120 nm. Control structures were also fabricated in which a pair of gold nanodisks were deposited on an unpatterned SiN surface. Dark-field scattering from such nanodiscs were studied using an inverted dark-field microscope equipped with an oil-immersion objective lens of numerical aperture 0.5.

To explore the effect of the NPs within the cavities, we have fabricated and studied two types of control devices. One control was based on an identical L3 cavity structure, however here the metal NPs were omitted from the fabrication process. We also explored the optical properties of the cavities after having deliberately removed the gold NPs. This was done using a nitric and hydrochloric acid etch, leaving the cavity structure intact but having two small holes on the cavity surface where the gold NPs had been.

All structures created were explored using optical spectroscopy. To excite the cavity / plasmon resonance, a 532 nm diode laser was collimated and then focused through a 100X long working distance microscope lens (numerical aperture 0.77) to a 2.5 μm diameter spot on the cavity surface. Here, scattered light from the NP dimer was collected using the same lens and passed through a polarizer and a long pass filter with a cut-off at 532 nm to reject the excitation laser light. The light was then imaged into a nitrogen cooled CCD spectrometer. To locate the cavity containing the gold NPs, a white light source was also used to illuminate the surface, with a flipper-mirror placed into the optical path directing light into a CCD camera.

To model the structures fabricated, we have used a finite difference time dependent (FDTD) model [25]. Due to computational constraints, the photonic crystal was limited in size to approximately (4×3.5) μm. The complex dielectric function of the gold dimer was described using a Drude-Lorentz model. To describe the hybrid plasmonic-photonic structure the cavity mode structure was first modelled without the presence of the gold dimer. A broadband dipole was placed in the cavity at a point 10 nm below the membrane surface at a point of low symmetry. Once the dipole had expired, the flux passing through a region above the L3 defect

was collected and used in our analysis. Once a suitable agreement with the emission from the empty cavity was obtained, the gold-dimer was placed into the cavity and the modelling repeated.

Discussion

A typical scattering spectrum recorded from a single pair of nanodisks separated by 70 nm is shown in Figure 1(c) (solid black line). It can be seen that there is an apparent scattering resonance that peaks at around 850 nm as expected for this type of structure. The dimer plasmon spectrum calculated with FDTD is also shown (dashed grey line). Here, the maximal E-field enhancement at the midpoint between dimers is monitored as a function of excitation wavelength, and shows a peak enhancement at the same wavelength as is observed in the experimental scattering spectrum. Although this resonance is positioned at longer wavelength than that of the optical modes supported by the cavity (typically located between 640 and 690 nm), the significant broadening of the plasmon results in some degree of overlap with the cavity modes.

Figure 2(a) plots the measured light emission of a typical 'empty' cavity. Here, luminescence from the cavity results from the weak, intrinsic luminescence from the SiN that is modified by the optical properties of the cavity. It can be seen that four optical modes are observed that we label M1 to M4, with M1 polarized in the y direction and M2 and M3 polarized in the x-direction. To confirm the origin of these modes, we used FDTD calculations to describe the structure as shown in figure 2(b). The agreement between the mode energies of the model and the experimental data is very good. Modes M3 and M4 appear relatively more intense in our calculations, however, this could be due to a number of factors including (i) the relative distribution of photoluminescence energy by the SiN dielectric, (ii) differences in the solid angle of light collection between the model and in the experiments and (iii) the effect of the position of the dipole in the model. The amplitudes of the x- and y-components of the electric-field distributions for each of the cavity modes are plotted in Figure 3.

The effect of the gold nanodisk dimers on the optical modes of the L3 nanocavity was explored by comparing the emission from a cavity either containing a dimer, or from the same cavity after the dimer had removed using an acid wash. Again, both FDTD calculations and experimental measurements were used to characterise the optical properties of the cavity as shown in Figure 4(a) (FDTD calculations) and 4(b) (experimental measurements). Here

data is presented for cavities having dimer separations of 40, 80 and 120 nm. It can be seen that the FDTD model makes four main predictions; (i) the amplitude of the optical modes are relatively suppressed by the inclusion of the metallic nanoparticles, (ii) mode M3 is strongly suppressed for small particle separations (see Supplementary Figure 1 for the modelled spectra of mode M3 only, with and without the dimer present), (iii) there is a general broadening of all modes (from around 3 nm to 8 nm), and (iv) a red-shift of mode M1. As we demonstrate below, the predicted suppression of mode M3 results from the fact that it is polarised in a direction parallel to that of the metal dimer axis (along the x-axis), and that the region of its highest field amplitude (at the centre of the cavity) coincides precisely with the gap between the two nanoparticles. At small particle separation therefore, coupling between the E_x field and the plasmon resonance is expected to be efficient, thus explaining its relatively strong suppression.

Our preliminary experimental measurements therefore confirm a general suppression of mode intensity in the cavities containing the metallic dimer accompanied by a general mode broadening; a result consistent with the FDTD model, with our measurements indicating that mode M3 is un-resolvable in all structures. Notably however, we do not observe a red-shift in mode M1. This discrepancy between model and experiment is not currently understood, however we note that the small scattering signal makes the identification of the peak wavelength of M1 difficult. In contrast, we observe a small blue-shift of mode M2 between 0.5 and 4 nm in cavities containing the NPs (dependent on NP separation). This is apparently confirmed by the model, which also suggests a blue-shift of around 2 nm is expected in cavities containing the MP dimer. In general however, we find (both experimentally and using our model) that the metallic dimer does not strongly modify the energy or spatial extent of the optical-modes within the cavity.

To quantify the interaction between the nanoparticle plasmon and the cavity, we follow previous methods [7] and explore modification to the cavity mode Q-factor in the presence of the metallic NPs. In particular, we use the FDTD model to explore how the cavity mode Q-factor changes as a function of dimer separation for modes M1 and M3. We note that previous work has confirmed that Q-factor is dependent on the relative orientation of the particles in the cavity [7], their position with respect to the EM field maxima within the cavity [13] and their relative separation. For both modes M1 and M3, we place a broadband dipole source at the centre of the cavity, y-polarized for M1 and x-polarized for M3, in order to selectively excite the mode. Once the dipole has decayed, the E-field at the cavity centre is

recorded as a function of time and a decay time is then extracted, allowing a Q-factor for the mode to be determined.

Figure 5 shows the time dependent E-field envelope for a series of dimer separations for mode M1 (a) and M3 (b). The graph insets show the calculated Q-factor for the respective modes. Note that since the simulation uses a spatially truncated photonic crystal, the Q-factors cannot be directly compared with those found experimentally. For the case of mode M1 we find that without the metallic nanoparticles present, the cavity Q-factor is calculated to be 1050. However on introduction of the nanoparticles, we find the lifetime of the mode is greatly reduced, dropping to approximately 300. It can be seen that the mode Q-factor is relatively insensitive to the dimer spacing, indicating that the drop in Q-factor is not due to interaction with the dimer plasmon. Instead, we suggest that the reduction in cavity lifetime when going from an empty cavity to a dimer-containing cavity is due to direct optical absorption without excitation of the dimer plasmon. This is expected, since the mode is polarized along the y-direction, which is unable to excite the collective dimer plasmon as it is x-polarised.

In contrast, mode M3 shows a clear relationship between mode lifetime and dimer spacing. We find that Q-factor of mode M3 in the empty cavity is ~360; a value that is reduced to a value of 150 at a dimer spacing of 30 nm. This relationship confirms that the dimer plasmon plays a direct role in the reduction of the cavity lifetime; a fact made possible since M3 is polarized in the x-direction, and has a field antinode at the cavity centre, and therefore has the same symmetry as the dimer plasmon. The relative change in the cavity lifetime upon the introduction of the dimers for modes M1 and M3 is shown in Supplementary Figure 2.We note that in the experimentally observed and calculated emission spectra of Figure 3(b), mode M3 is strongly suppressed in the presence of the dimer, further confirming this nature of this interaction.

We have also modelled the relative intensity of the E-field between the dimers when they are printed onto the cavity as a function of their separation. Again, the cavity was resonantly excited with a cw dipole at the cavity centre having an x- or y-polarisation to excite either the M3 or M1 mode respectively. The simulation was run until the E-field amplitude as measured between the gold nanoparticles converged to a constant value. Interestingly, we find that without the cavity, the dipole is unable to directly excite the dimer plasmon. As can be seen in Figure 5(c), we find that for mode M3, the EM field between the dimers is enhanced

significantly at small particle separation and decreases with increasing separation. This indicates that cavity mode M3 can indeed drive the dimer plasmon, In contrast, the intensity of the EM field between dimers following resonant excitation of mode M1 is attenuated at small particle separations, indicating that this mode does not excite the plasmon. The E-field instead increases with increasing dimer separation; an effect that we speculate results from the fact that at dimers small separations physically block or absorb light that leaks from the cavity mode.

Conclusion

Our results suggest that orienting a plasmonic nano dimer parallel to the photonic field polarization can create an electromagnetic hot spot between dimers having a relatively small separation. This suggests therefore that the hybrid metallic dimers / PC nanocavity system could be used as a platform to fabricate optical devices to create a high near-field intensity which could potentially be used to control light-matter interactions at nanometre length scales. We speculate therefore that the structures fabricated here may form the basis of new types of plasmonic/photonic laser. Our study predicts a field enhancement between gold nanodisks can be achieved when they are introduced into an L3 nanocavity. This is anticipated to result in a large Purcell factor between the dimer. The enhancement could be used to increase the radiative rate of an optically-active semiconductor material (e.g. an organic semiconductor [26], or quantum dot ensemble [27]), placed within the cavity at a point corresponding to a local field maxima, while the cavity acts as a high-Q resonator to provide feedback for the emitted photons. Here, our structures that both enhance local EM-fields and provide defined optical feedback could be used to reduce lasing thresholds.

Acknowledgements

We thank the UK EPSRC for funding this work through the Programme Grant ‘Hybrid Polaritonics’ EP/M025330/1. K.N.S. thanks the Kurdistan Regional Government for the provision of a research studentship. We also thank William Barnes and Alastair Humphrey at the University of Exeter for dark-field scattering measurements on metal NP dimers.

References

[1] S. A. Maier, Springer Science Business Media LLC (2007).

[2] J. F. Li, Y. F. Huang , Y. Ding, Z. L. Yang , S. B. Li , X. S. Zhou , F. R. Fan, W. Zhang, Z. Y. Zhou , D. Y. Wu1 , B. Ren , Z. L. Wang and Z. Q. Tian, Nature Letters, 464, (2010).

[3] J. N. Anker, W. P. Hall, O. Lyandres, N. C. Shah, J. Zhao and R. P. Van Duyne, Nature Materials, 7, (2008).

[4] V. Giannini, A.I. Fernandez-Dominguez, Y. Sonnefraud, T. Roschuk, R. Fernandez-Garcia, and S.A. Maier, Small. vol. 6, no. 22, Nov 22. 2010, pp. 2498-2507.

[5] S. Link and M.A. El-Sayed, Journal of Physical Chemistry B. vol. 103, no. 21, May 27. 1999, pp. 4212-4217.

[6] Kelly KL, Coronado E, Zhao LL, Schatz GC (2003) J Phys Chem B 107:668

[7] M. Barth, S. Schietinger, S. Fischer, J. Becker, N. Nüsse, T. Aichele, B. Löchel, C. Sönnichsen, and O. Benson, Nano Letters, 10, 3, 891– 895 (2010).

[8] T. Zhang, S. Callard, C. Jamois, C. Chevalier, D. Feng, and A. Belarouci, Nanotechnology, vol. 25, no. 31, Article ID 315201, 2014.

[9] F. De Angelis, M. Patrini, G. Das, I. Maksymov, M. Galli, L. Businaro, L. C. Andreani, and E. Di Fabrizio, Nano Letters, 8, 8, 2321–2327 (2008).

[10] M. Barth, N. Nusse, B. Lochel and O. Benson, Optics Letters, 34 1108–1110 (2009).

[11] I. Mukherjee, G. Hajisalem, and R. Gordon, Optics, Express 19, 23, 22462–22469 (2011).

[12] M. Barth, J. Stingel, J. Kouba, N. Nusse, B. Lochel, O. Benson, Phys. Status Solidi B 246, 298-301 (2009).

[13] Y. Yi, T. Asano, Y. Tanaka, B-S Song, and S. Noda, Optics Letters, 39, 19, 5701-5704 (2014).

[14] M.W. McCutcheon and M. Loncar, Optics Express, 16, 23, 19136 (2008).

[15] Y-J Fu, Y-S Lee, and S-D Lin, "Design and demonstration of high quality-factor H1-cavity in two-dimensional photonic crystal", Optics Letters, 38, 22, (2013).

[16] T. Tanabe, A. Shinya, E. Kuramochi, S. Kondo, H. Taniyama and M. Notomi, Applied Physics Letters, 91, 021110 (2007).

[17] A.M. Adawi, M.M. Murshidy, P.W. Fry, and D.G. Lidzey, ACS Nano, 4, 6, 3039-3044 (2010).

[18] B. Ellis , M. A. Mayer, G. Shambat, T Sarmiento, J. Harris, E. E. Haller, J.Vuckovic, Nature Photonics, 5 , 297-300 (2011).

[19] M. D. Birowosuto, H. Sumikura, S. Matsuo, H. Taniyama, P. J. van Veldhoven, R. Notzel, M. Notomi, Scientific Reports, 2, 321, (2012).

[20] K. Deasy, K. Sediq, S. Brittle, T. Wang, F. Davis, T. Richardson and D.G. Lidzey, Journal of Materials Chemistry C 2, 8700–8706 (2014).

[21] W. M. Wang, R. M. Stoltenberg, S. Liu, and Z. Bao, ACS Nano Vol. 2 · No. 10, 2135–2142 (2008).

[22] P. Manandhar, J. Jang, G. C. Schatz, M. A. Ratner, and S. Hong, Physical Review Letters, Vol 90, No. 11, (2003).

[23] J. Do, K. N. Sediq , K. Deasy , D. M. Coles , J. Rodríguez-Fernández, J. Feldmann, and D.G. Lidzey, Advanced Optical Materials, 1, 946–951 (2013).

[24] H. Aouani, J. Wenger, D. Gerard, H. Rigneault, E. Devaux, T. W. Ebbesen, F. Mahdavi, T. Xu, and S. Blair, American Chemical Society Nano, 3, 7, 2043–2048 (2009).

[25] A. F. Oskooi, D. Roundy, M. Ibanescu, P. Bermel, J. D. Joannopoulos, and S. G. Johnson, Computer Physics Communications, 181, 687–702 (2010).

[26] J. R. Lawrence, G. A. Turnbull, and I. D. W. Samuel, Applied Physics Letters, 80, 3036 (2002).

[27] H. Chang, K. Min, M. Lee, M. Kang, Y. Park, K-S Cho, Y-G Roh, S. W. Hwang and H. Jeon, Nanoscale, 8, 6571 (2016).

Figure captions

Figure 1: Part (a) shows a schematic of a L3 nanocavity containing a gold nanoparticle dimer. Part (b) shows a typical SEM image recorded from a nanocavity containing such a nanoparticle dimer. The scale bar is 500 nm. Part (c) shows a dark-field scattering spectrum of a gold nanoparticle dimer on an unpatterned silicon-nitride membrane surface (solid black line). Here, the gold nanoparticles were separated by 70 nm. The dimer plasmon spectrum as calculated by FDTD is also shown (dashed grey line).

Figure 2: Part (a) shows a typical PL emission spectrum from an 'empty' L3 nanocavity defined into a silicon nitride membrane. We identify modes M1 to M4 as discussed in the text. Part (b) shows the simulated emission from such a nanocavity calculated using an FDTD model.

Figure 3: The amplitude of the E-field polarised in the x and y directions for modes M1 to M4.

Figure 4: Parts (a) to (c) show the results of FDTD modelling of cavity emission for cavities either containing a gold nano-particle dimer (red-line) or for cavities having a surface containing two small recesses (10 nm deep, long-axis of 160 nm and aspect ratio of 1.53) (black-line). Data is plotted for cavities in which the recess separation is 40, 80 and 120 nm respectively. Parts (d) to (f) plot experimental-measured emission spectra for the cavities modelled in parts (a) to (c). Here, the red-line corresponds to cavities containing a gold nanoparticle dimer. The spectra shown using the black line was recorded from the same cavities after the gold nanoparticles had been removed using an acid wash.

Figure 5: Parts (a) and (b) shows the FDTD calculated time dependent E-field envelope for a series of dimer separations (indicated in the figure) for mode M1 and M3 respectively. The graph insets show the calculated Q-factor for the respective modes. Part (c) shows the FDTD calculated EM field between the dimers as a function of separation for modes M3 and M1 (plotted using red and black symbols respectively).

Figure 1

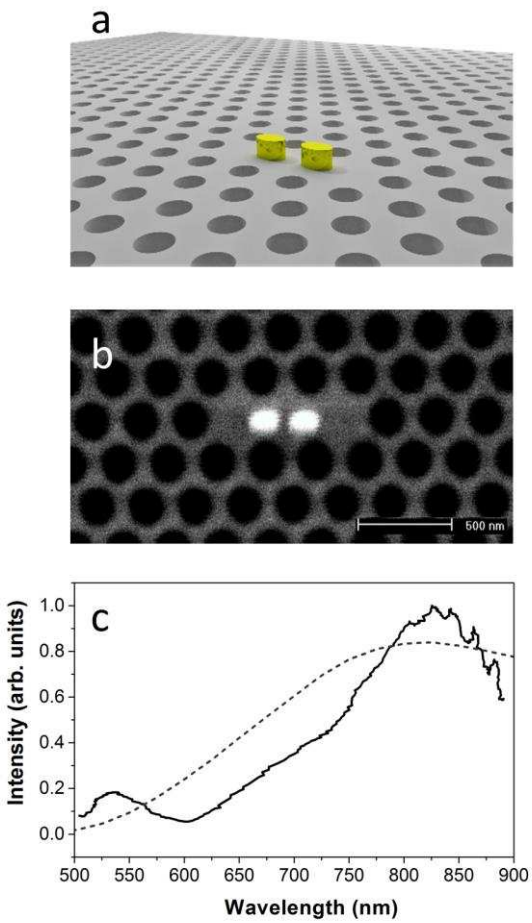
a
b
500 nm
c
Intensity (arb. units)
1.0
0.8
0.6
0.4
0.2
0.0
500
550
600
650
700
750
800
850
900
Wavelength (nm)

Figure 2

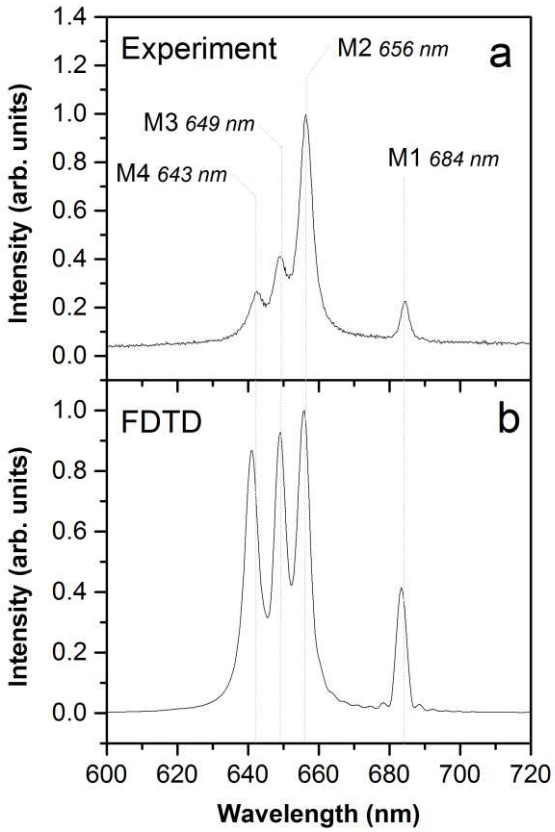
Experiment
M2 656 nm
a
M3 649 nm
M1 684 nm
M4 643 nm
Intensity (arb. units)
FDTD
b
Intensity (arb. units)
Wavelength (nm)

Figure 3

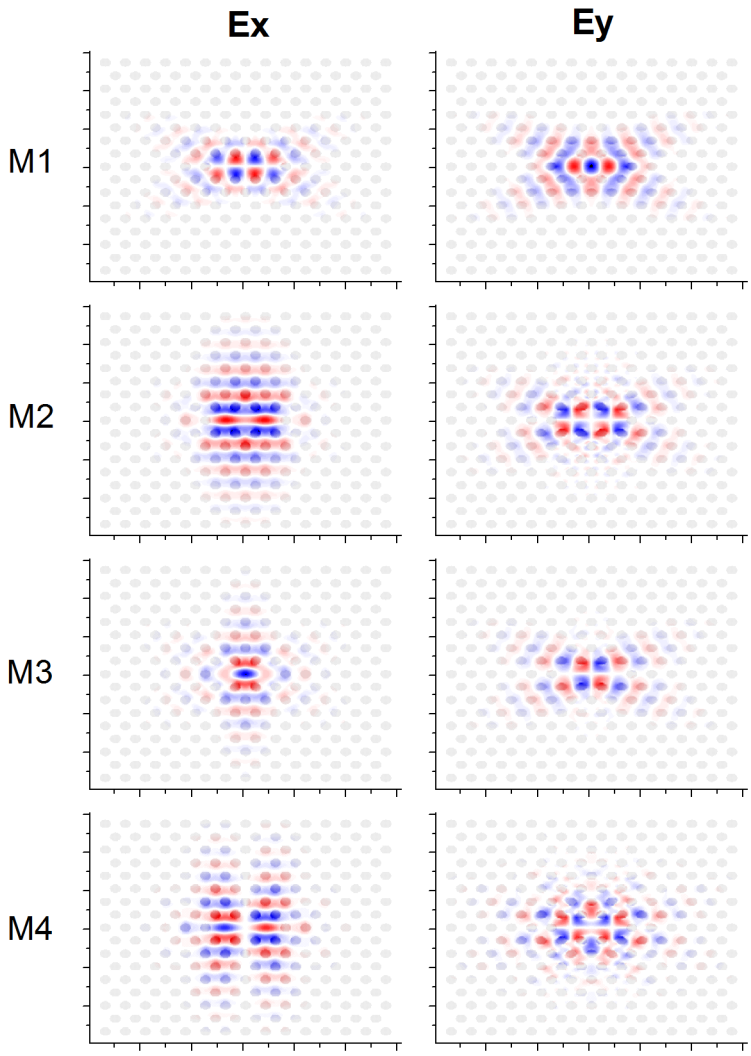

Figure 4

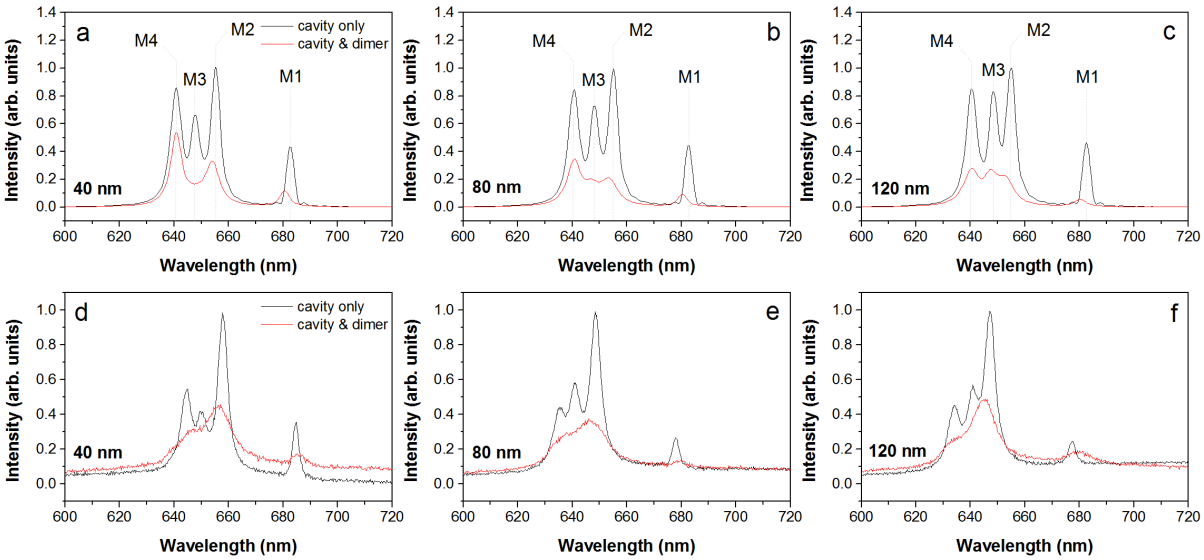
a
b
c
d
e
f
M1
M2
M3
M4
cavity only
cavity & dimer
40 nm
80 nm
120 nm
Intensity (arb. units)
Wavelength (nm)

Figure 5

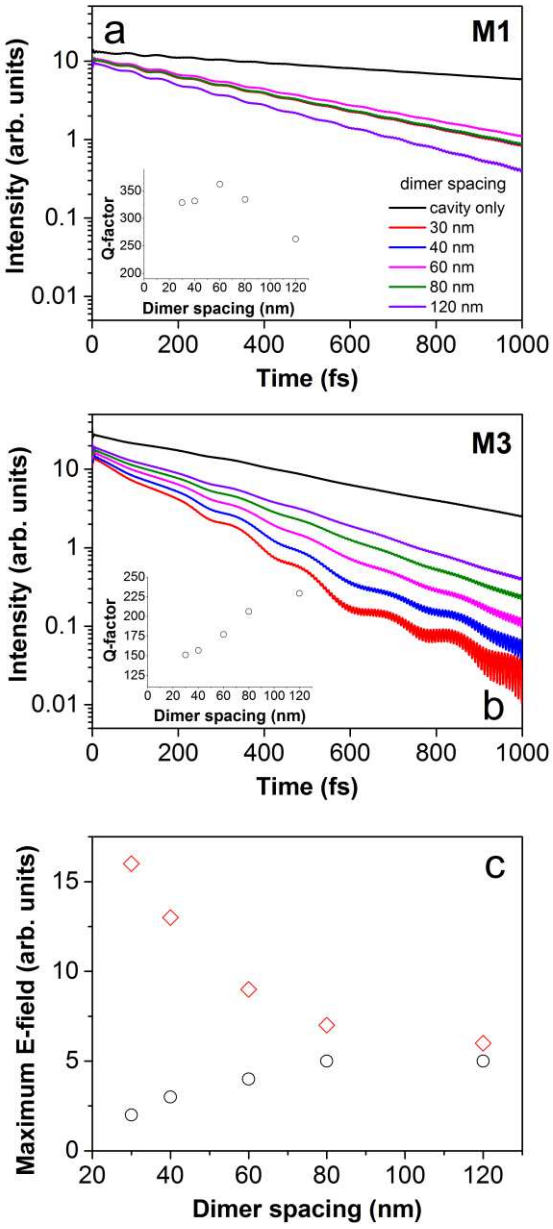
a
M1
Intensity (arb. units)
10
1
0.1
0.01
0
200
400
600
800
1000
Time (fs)
dimer spacing
cavity only
30 nm
40 nm
60 nm
80 nm
120 nm
Q-factor
350
300
250
200
0 20 40 60 80 100 120
Dimer spacing (nm)
M3
b
250
225
200
175
150
125
c
Maximum E-field (arb. units)
15
10
5
0
20
40
60
80
100
120
Dimer spacing (nm)